RSC Advances

ROYAL SOCIETY OF CHEMISTRY

www.rsc.org/advances

Journal Name

ARTICLE

Aggregation kinetics and cluster structure of amino-PEG covered gold nanoparticles

Received 00th January 20xx,
Accepted 00th January 20xx

DOI: 10.1039/x0xx00000x

www.rsc.org/

D. Zámbó,[a] Sz. Pothorszky,[a] D.F. Brougham[b] and A. Deák[a]

In this study controlled clustering kinetics is demonstrated for PEG grafted gold nanoparticles, in response to applied environmental stimuli; the temperature and ionic strength of the medium. It is also found that the rate of assembly determines the structure of the prepared clusters. After the system is brought out of equilibrium, time-dependent extinction and dynamic light scattering data are used to follow the evolution of nanoparticle cluster formation in real time. The results show that the rate of assembly increases with increasing ionic strength or temperature of the medium. As a result the nanoparticle cluster size scales with ionic strength and temperature, over a cluster size range from a few particle sizes up to the micron-scale. It is found that, even at the lowest ionic strength, the electric double layer repulsion is eliminated; hence the observed differences in kinetics and in cluster structure arise from modulation of the repulsive steric interactions between nanoparticles. The approach should be extendable to suspensions of other nanoparticle types, where the nanoparticle stability is determined by surface-grafted responsive macromolecules.

Introduction

Nanoparticle clusters (NPCs) prepared from self-assembled nanoparticles can open up new routes towards numerous special applications due to emerging collective properties. The clusters can be efficiently used in sensors,[1] surface enhanced Raman scattering (SERS)[2-5] or organic photovoltaic devices.[6] Gold nanoparticles are excellent candidates for building bigger hierarchical structures, firstly because the size and shape can be well controlled.[7,8] Secondly, as a result, their optical response can be tuned as it is determined by interparticle coupling. Thirdly, their aggregation can be monitored using simple visible light spectroscopy, due to pronounced spectral changes upon plasmon coupling between the NPs.[9-11] Finally, the surface of gold nanoparticles can be easily modified by a number of molecules, e.g. thiol containing polymers,[12-13] opening up a wide range of possibilities for post synthesis functionalization. Due to the wide range of molecules, which can be immobilized on the gold nanoparticles' surface, the formation of clusters is feasible by cross-linking,[14,15] phase separation (emulsion) techniques,[2] using colloidal forces such as exploiting the solvophobic feature of the ligands,[16] electrostatic double layer interactions[17-19] or based on the responsive properties of surface grafted molecules[20-21] following application of an external stimulus. Responsive colloidal forces are attractive to drive nanoparticle assembly as both the colloidal stability and the stimulus-response is ensured by a single surface agent, as a result the stability of the clusters in an application-relevant environment can be designed.

Formation of ordered NPCs from homogeneous media (i.e. from a dilute nanoparticle solution) is challenging, because these processes require highly monodisperse building blocks as well as control over the colloidal interactions. Klotsa *et al.* have shown that for NPC preparation from dilute suspension, the optimal process is a balance between driving force and kinetic accessibility. Based on their calculations, for the successful preparation of compact NPCs a 'soft-sphere' type interaction potential is required with an energy depth around 2-3 kT.[22] This implies, that the assembly process is in general highly depends on the balance between competing colloidal interactions. Accordingly, cluster formation can be controlled by modulating the net interparticle interactions *i.e.* by varying the depth of the energy minimum for a given 'soft-sphere' type interaction. This type of interaction energy curve can be engineered by using surface adsorbed polymer chains, that can counterbalance the van der Waals attraction but only at small particle-particle separation distances.[23] Poly(ethylene glycol) derivatives are often used as stabilizers for gold nanoparticles because of their biocompatibility, stealth action, their potential multiple chemical functionality (upon modification) and their ease of grafting due to the high affinity of thiol or amino groups to the gold surface.[24-28] We have recently demonstrated that PEG chains can also be used as a thermoresponsive surface coating at sufficiently high ionic strengths to trigger the clustering of gold particles.[23]

[a] Institute for Technical Physics and Materials Science, HAS Centre for Energy Research, P.O. Box 49, H-1525 Budapest, Hungary
[b] School of Chemistry, University College Dublin, Belfield, Dublin 4, Ireland
† Footnotes relating to the title and/or authors should appear here.
Electronic Supplementary Information (ESI) available: [details of any supplementary information available should be included here]. See DOI: 10.1039/x0xx00000x

In this paper we show how this process can be fine-tuned by adjusting two easily controlled environmental parameters (temperature and ion concentration) that affect the clustering process (kinetics and NPC structure) through modulating colloidal interactions (see Scheme 1). We demonstrate these effects with controlled assembly of amino-PEG-coated gold nanoparticles. The nanoparticle clustering process was followed by time-dependent dynamic light scattering, DLS, and visible light spectroscopy, and the resulting cluster structures were analysed by scanning electron microscopy. It is shown that the PEG-determined steric interaction can be continuously tuned allowing fine control over the net colloidal interaction. This is turn allows the rational design of colloidal building blocks for the controlled preparation of compact NPCs from dilute solutions.

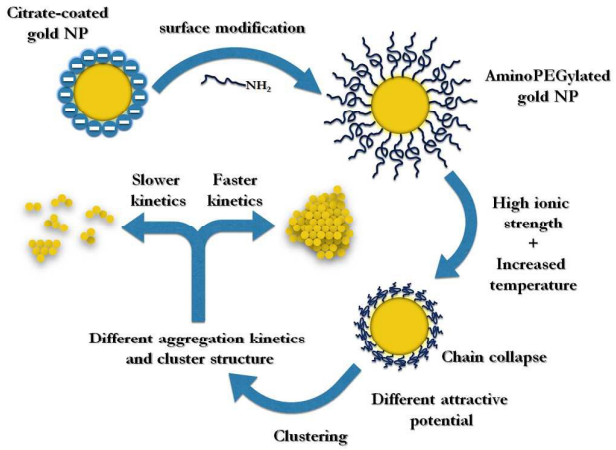

Scheme 1. Outline of the process, resulting in different outcomes of the assembly process depending on the external stimulus.

Experimental section

Synthesis and surface modification of gold nanoparticles

Tetrachloroauric acid trihydrate ($HAuCl_4 \cdot 3H_2O$; 99.9%), sodium citrate tribasic dihydrate (ACS reagent, ≥99.0%) and potassium sulphate (ReagentPlus®, ≥99.0%) were obtained from Sigma-Aldrich. Methoxy-ω-amino poly(ethylene glycol) (mPEG-NH_2; MW of 2000 Da) was supplied by Rapp Polymere GmbH. All chemicals were used as received. Ultrapure water with a resistivity of 18.2 MΩ·cm was used in all experiments.

Gold nanoparticles were synthesized by the traditional Turkevich method,[29] which resulted in citrate stabilized nanoparticles with narrow size distribution. 6 mL of 0.01 M $HAuCl_4$ trihydrate solution was added to 222 mL of Milli-Q water and heated to boil on a hot plate under vigorous stirring. When the solution started to boil, 6 mL of 38.76 µM sodium citrate solution was added. The solution was boiled continuously for 15 minutes, where through the colour of the system changed to ruby red. After this, the sol was allowed to cool down to room temperature.

Surface modification of gold nanoparticles was carried out by dissolving 200 mg of mPEG-NH_2 (MW = 2000 Da) in 1 mL of Milli-Q water by sonicating the solution, and adding to 20 mL of gold nanoparticle sol. After reacting for 3 hours on an orbital shaker, the samples were cleaned by centrifuging (9500 RCF, 30 min) and redispersed in Milli-Q water. The polymer grafted nanoparticles could be stored at room temperature in plastic centrifuge tubes in the dark for months. After the synthesis and surface modification the final concentration of the nanoparticles (0.69 nM; $4.16 \cdot 10^{11}$ NPs/mL) was determined from the visible light spectra.[30]

Nanoparticle assembly monitoring and cluster evaluation

Conventional and time-dependent DLS measurements were carried out using a Malvern ZetaSizer Nano ZS device. For temperature trend DLS measurements the samples were heated from 25 to 70 °C in 5 °C steps. DLS data were collected at the different temperatures, after allowing the sample to reach thermal equilibrium for 5 min after each temperature change.

For time-dependent measurements the aqueous solution of the PEGylated Au NPs was heated to 50 and 60 °C, which were chosen based on the temperature trend DLS measurements. The clustering process was initiated by rapidly injecting 500 µL of pre-heated K_2SO_4 solution with appropriate concentration into 500 µL of nanoparticle sol of the same temperature. DLS data were collected with 1 minute resolution. Visible spectra were recorded using a fibre coupled spectrometer (ThorLabs CCS 200 Compact CCD Spectrometer) in a temperature controlled cuvette holder, with 1 second resolution for the first 15 minutes, then 10 seconds resolution was used for the next 30 minutes.

To prepare samples for SEM measurements, the reaction was performed in a disposable cuvette, which contained a silicon wafer at the bottom in order to collect gold aggregates after the clustering was allowed to proceed for 45 minutes. Scanning electron microscopy was carried out using a Zeiss Supra micro-scope operated at 5 kV acceleration voltage. The SEM images of the clusters were analysed using open source software (ImageJ). The SEM images were calibrated based on the SEM scale bars and converted to 8-bit grey scale images. Careful thresholding was carried out until the best outline match of the objects was achieved. The images were inverted and the perimeter of the identified objects was extracted in nanometres.

Results and discussion

Characterisation of gold nanoparticles

Physical characterization of the NP suspensions during the surface preparation process, including extinction spectra, size distributions, and ζ-potential values recorded before and after PEGylation are presented in Figure 1. The LSPR peak position of citrate stabilized gold nanoparticles was slightly red shifted (from 516 to 518 nm) by the presence of mPEG molecules in the near field of the particles. The samples have narrow size distribution; the mean hydrodynamic size increased on surface modification from 20.0 ± 0.2 to 29.7 ± 0.2 nm. The ζ-potential changed from ca. -42 to -18 mV. The negative charge

remaining on the particles can be attributed to the presence of chloride ions on the nanoparticles surface, which are remains from the NP synthesis involving $HAuCl_4$ salt.[31] The suspension remained stable after purification using Eppendorf MiniSpin benchtop centrifuge (9000 RCF, 30 min), and could also be transferred to polar organic solvents; EtOH, $CHCl_3$ (see Supporting Information Figure S2).

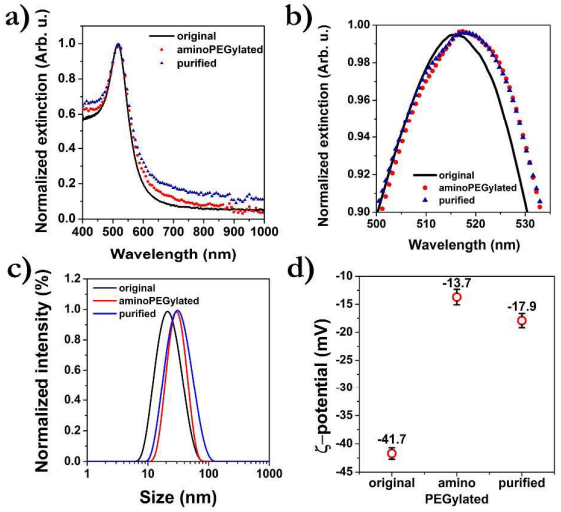

Figure 1. a) Extinction spectra, b) LSPR peak positions, c) DLS size distributions and d) zeta potential of the nanoparticle suspensions before and after PEGylation.

Perturbation induced clustering of gold nanoparticles

The size distribution of the system as a function of temperature was investigated using DLS measurements to determine the temperature threshold of the clustering process.[23] It should be emphasized that, in contrast to previous results obtained for thiol-PEG grafted particles in the presence of 2 M (or higher) NaCl,[32] our starting suspensions containing K_2SO_4 at up to 0.3 M are perfectly stable (See Supporting Information Figure S3). Hence spontaneous desorption of the PEG molecules under these conditions can be ruled out. The measured intensity distributions are collated in Figure 2.

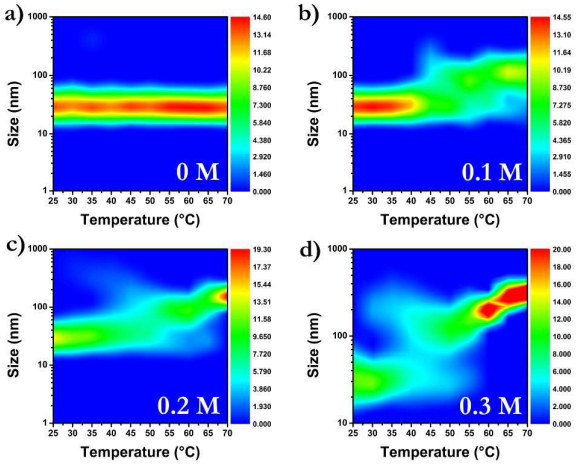

Figure 2. DLS size distribution as a function of temperature at different K_2SO_4 concentrations.

In this representation, values along any vertical slice (at a given temperature) correspond to the conventional DLS intensity distribution; so for instance in Figure 2a the red band corresponds to the size of the maximum in the distribution. When no electrolyte is added, the original size distribution of the individual particles is retained over the whole investigated temperature range (Fig. 2a). In the presence of salt (Fig. 2b-d), however, clustering of nanoparticles can be observed, with a temperature threshold that decreases with increasing electrolyte concentration (from 45 to 35 °C, for 0.1 and 0.3 M K_2SO_4, respectively). The change in size is very pronounced on increasing the temperature from 50 to 60°C in this range of ionic strengths. Hence the time dependence of spectral properties of the suspensions, following perturbation, were investigated at these two temperatures to shed light on differences in the kinetics of assembly at different ionic strengths. The time-dependent extinction spectra for four model suspensions; two salt concentrations (0.2, 0.3 M K_2SO_4) and two temperatures (50, 60 °C), are shown in Figure 3.

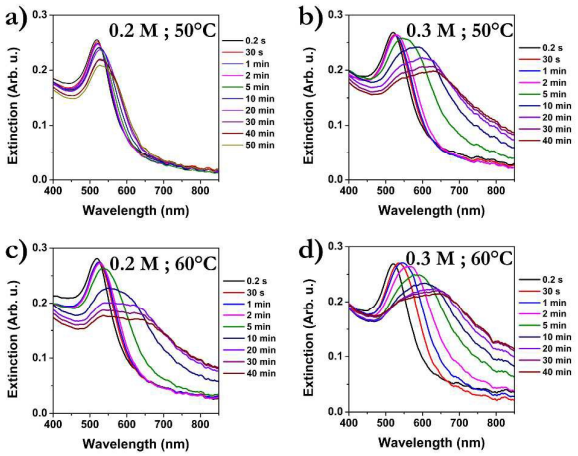

Figure 3. Time evolution of the extinction spectra for amino-PEGylated gold nanoparticles at different K_2SO_4 concentrations and temperatures; a) 0.2 M and 50 °C; b) 0.3 M and 50 °C; c) 0.2 M and 60 °C; d) 0.3 M and 60 °C.

The spectral changes observed at 50 °C depend heavily on the electrolyte concentration. At 0.2 M the LSPR peak of the particles broadens in time with a minor indication of a shoulder around 570 nm, that could be due to the appearance of a small fraction of clusters composed of a few particles only.[10,33] At 0.3 M for the first two minutes the extinction peak redshifts, however subsequently a second peak starts to evolve (Figure 3c), which increases in intensity with time and stabilizes ca. 630 nm. We assign this to a cluster mode, shifted due to plasmon coupling between particles in the clusters, which increases in intensity as the number of interactions increase over time. Similar behaviour can be observed for 0.2 M and 60 °C (Figure 3b). For the suspension exposed to both higher ionic strength and temperature (0.3 M and 60 °C) major changes in the extinction spectra occur during the first 2

minutes; with red-shifting and significant broadening which continue to evolve more strongly over the subsequent 38 mins. This suggests faster aggregation kinetics in this case.

Time-dependence of clustering

In order to investigate the differences in the kinetics of assembly for the four model suspensions, extinction values were extracted and plotted as a function of time at two characteristic wavelengths; the LSPR peak wavelength of the original nanoparticles (518 nm) and at a wavelength corresponding to the evolving coupled mode (630 nm). For 0.2 M and 50°C the coupled feature is not resolved, so we have used the extinction values extracted for the minor shoulder in the spectrum at 570 nm (Figure 4a). In all cases, the slow decrease of the original LSPR peak intensity can be attributed to a decrease in the number of free particles due to their incorporation into clusters. The clustering process becomes faster at higher salt concentration (0.3 M) at 50 °C (Figure 4b). For 0.2 M and 60 °C (Figure 4c) a similar decay profile can be observed. At 60 °C and 0.3 M salt concentration (Figure 4d) the spectra suggest that the initial aggregation rate is significantly higher. In particular the sudden extinction decay (at 518 nm) shows that aggregation starts within seconds on increasing the ionic strength.

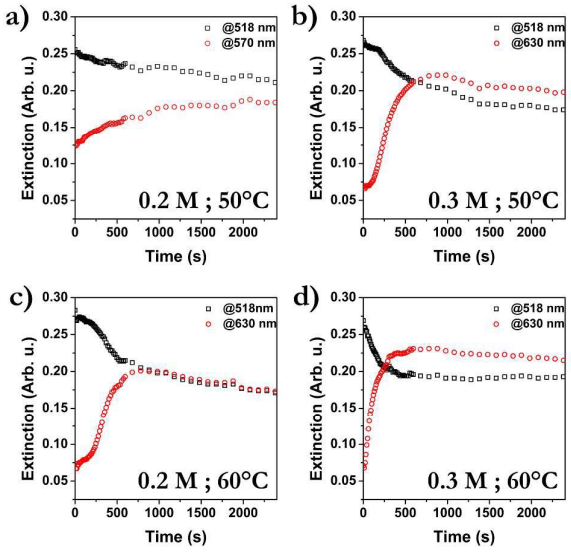

Figure 4. Time-dependent extinction decay plots for amino-PEGylated gold nanoparticles as measured at characteristic wavelength values for different temperatures and salt concentrations; a) 0.2 M and 50 °C; b) 0.3 M and 50 °C; c) 0.2 M and 60 °C; d) 0.3 M and 60 °C.

The size evolution of nanoparticle clusters was also followed by time dependent DLS (Figure 5), which confirms the differences in the aggregation kinetics suggested by the extinction spectra. The time evolution of the mean hydrodynamic size, d_{hyd}, and the count rate for the four model suspensions are shown in Figure 6. For 0.2 M and 50 °C (Figure 6a) a slight increase in d_{hyd} is observed over time. The associated increase in the scattering intensity is expected given the strong dependence of intensity on size, which reflects the fact that the d_{hyd} value is strongly weighted to the larger scatterers in the distribution. On increasing either the concentration or temperature a more rapid increase in d_{hyd} is observed with an initial increase in the count rate (Figure 6b,c). This is followed for both suspensions by a transition point at ca. 300-500 s, after which the count rate starts to decrease, which we assign to sedimentation of larger clusters. Hence the rate of increase in d_{hyd} is also slightly reduced in this stage. The response of the suspension at 0.3 M and 60 °C (Figure 6.d) is unusual; due to the very rapid aggregation only sedimentation (count rate decrease) can be observed by DLS. Over the parameter range studied the d_{hyd} value increases with temperature and ionic strength, with the latter having a stronger effect.

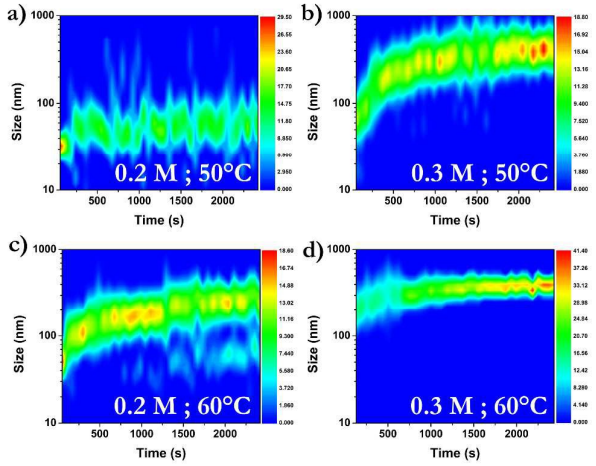

Figure 5. Time dependent dynamic light scattering contour plots displaying the measured size distribution as a function of time at different temperatures and salt concentrations; a) 0.2 M and 50 °C; b) 0.3 M and 50 °C; c) 0.2 M and 60 °C); d) 0.3 M and 60 °C.

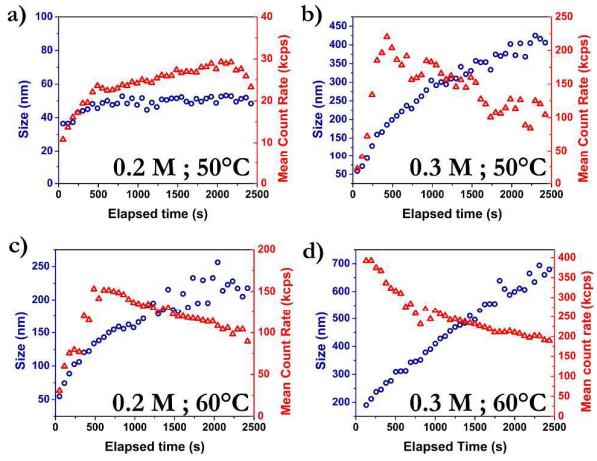

Figure 6. Average size and mean count rate measured by DLS as a function of time at different temperatures and salt concentrations; a) 0.2 M and 50 °C; b) 0.3 M and 50 °C; c) 0.2 M and 60 °C); d) 0.3 M and 60 °C. Blue circles represent the average sizes; red triangles represent the mean count rate values.

Structure of the nanoparticle clusters

Electron micrographs of samples removed from the four model suspensions after 40 minutes of assembly are shown in Figure 7. Different cluster sizes and structure can be observed depending on the ionic strength and temperature used during the assembly process (confirming the persistence of the structures). The mean size of the nanoparticle clusters increases with the temperature and electrolyte concentration and the number of individual nanoparticles decreases significantly. Small compact clusters formed from only a few particles are observed for the sample treated at 0.2 M and 50 °C. This is in good agreement with spectral features of this system, *i.e.* only broadening of the plasmon peak can be observed with a minor shoulder around 570 nm, with a very slight increase in d_{hyd}. As the temperature and the salt concentration are increased, the cluster size also increases dramatically in accordance with the DLS and extinction spectroscopy data. It has to be noted that the cluster sizes observed in SEM exceed the DLS values. This is due to the larger clusters being overrepresented in the SEM sample at the end of the clustering process compared to DLS due to sedimentation, which is in accordance with the observed drop in the count rates for all sets of parameters in Figure 6. In order to provide a (semi-)quantitative analysis of the change in cluster size, image analysis was performed on low-magnification (1k) images.

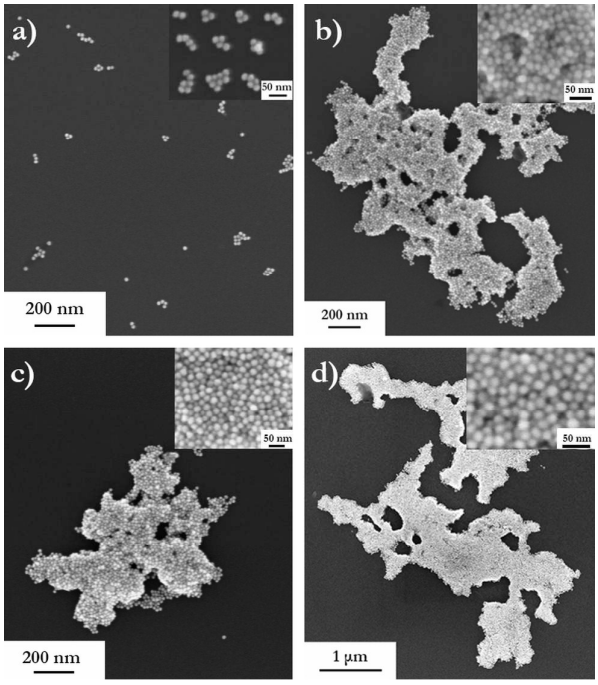

Figure 7. Structure of the gold nanoparticle clusters evolved after 40 minutes under different experimental conditions (K_2SO_4 concentration and temperature): 0.2 M and 50 °C (a); 0.3 M and 50 °C (b); 0.2 M and 60 °C (c); 0.3 M and 60 °C (d). Insets show the compact alignment of nanoparticle building blocks.

The distribution of the cluster perimeters, in nanometres, is shown in Figure 8. It is clear, that for this set of parameters, the ionic strength has a more determining effect on the cluster size, while there is also a significant, though smaller, difference as the temperature changes for a given ionic strength. This structural difference between the four sets of parameters can be interpreted in term of the different interaction potential between the nanospheres featuring a 'soft-sphere' type interaction energy curve.[22] Based on earlier results[23] the electric double layer repulsion between the particles is completely eliminated already at 0.2 M salt concentration and steric repulsion originating from the PEG chains is responsible for the colloidal stability of the system. At increasing temperature, the decrease in the steric repulsion and the developing 'soft-sphere' type interaction provides the necessary driving force for the clustering process. The findings presented here show that by varying the ion concentration and temperature, one can fine-tune the steric interaction. Although it should be noted that the hydrophobic interaction between the surface grafted polymers may also play a role,[34] increasing the attraction between the nanoparticles at smaller separations, thus it can contribute to the aggregation of the NPs.

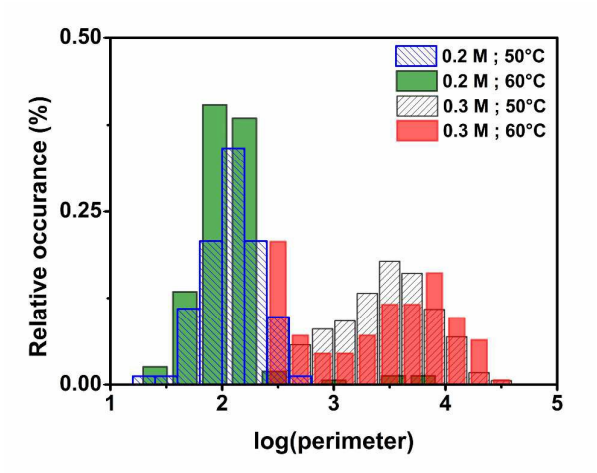

Figure 8. Effect of the different temperatures and ion con-centration on the resulting clusters. The perimeter of the aggregates in nanometer was obtained from image analysis analysing 200 clusters.

The compact nature of the observed NPCs, see insets to Figure 7b-d, indicates that, in accordance with the spectroscopic and DLS investigations, the process is not diffusion limited, and hence there should be only a moderate attraction between the NPs within the cluster. This interpretation is confirmed by investigating the stability of the smallest (0.2 M; 50 °C) and largest (0.3 M; 60 °C) NPCs. Suspensions were allowed to assemble for 600 seconds, and the clustering process was quenched by dipping the sample into ice cold water, after which ultrasonication was applied for 3 or for 5 minutes for different samples. The size distribution was then measured by DLS (Figure 9). For the small clusters (Figure 9a) a feature corresponding to the individual particles, at around 20 nm, appears after 5 minutes, showing successful (even if only partial) disassembly of the clusters. Additionally, for the present systems the presence of any force field that would self-limit the NPC growth[35] can be excluded and cluster-

to-cluster aggregation must also play a role in the growth process indicated by the irregular shape of the large clusters (Figure 7c-d). These observations point to a relatively weak attraction between the particles at 0.2 M and 50 °C, hence they form smaller clusters during the assembly and are more susceptible to forced disassembly upon sonication. This is consistent with the work of Kim *et al.*[9], which suggests higher stability ratios for colloids exhibiting weaker interparticle attraction during the aggregation process. For the larger clusters (Figure 9b), however, only fragmentation of the large aggregates occurs without the appearance of a significant number of monomers particles, indicating a more stable cluster and hence stronger attraction between the particles.

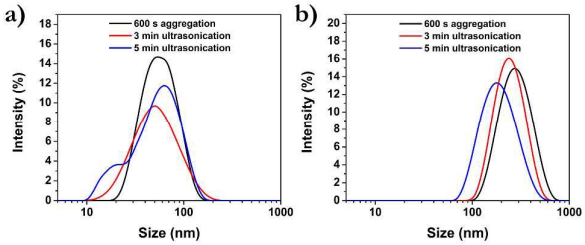

Figure 9. Effect of sonication on the DLS response for sus-pensions obtained after assembly for 600 seconds at (a) 0.2 M; 50 °C and (b) 0.3 M; 60 °C.

Conclusions

In summary, a tunable clustering process for amino-PEGylated gold nanoparticles is presented, where the structure of the nanoparticle clusters (NPCs) and the aggregation kinetics can be controlled by the ionic strength and the temperature of the medium. For different sets of parameters, entirely different NPC structures evolved over time, which can be attributed to the modulation of the steric repulsion arising from the PEG grafts. When the driving force for the clustering is smaller, only NPCs composed of a few particles are formed which can be effectively disassembled by providing external energy e.g. by ultrasonication. As the driving force increases, faster assembly occurs resulting in compact 3D assemblies. This suggests a proper soft-sphere type interaction energy profile, however, the size of the aggregates is significantly larger due to cluster-to-cluster aggregation. In the latter case, the NPCs undergo only partial fragmentation on ultrasonication; the individual particles cannot be recovered upon disassembly, indicating increased cluster stability with increasing size.

Acknowledgements

Authors thank Dániel Szekrényes for his help in the experimental part of the work and Levente Illés for the SEM images. This work received funding from the European Union's Seventh Framework Programme for research, technological development and demonstration under the project UNION, Grant N° 310250. The project was supported by the Hungarian Research Fund "OTKA-PD-105173" and "K-112114". A.D acknowledges the support of the János Bolyai Research Fellowship from the Hungarian Academy of Sciences. D.Z. and SZ.P. acknowledge the support of the Pro Progressio Foundation and József Varga Foundation.

Notes and references

1 L. Polavarapu, J. Pérez-Juste, Q.-H. Xu and L. M. Liz-Marzán, *J. Mater. Chem. C*, 2014, **2**, 7460–7476.
2 N. Pazos-Perez, C. S. Wagner, J. M. Romo-Herrera, L. M. Liz-Marzán, F. J. García de Abajo, A. Wittemann, A. Fery and R. A. Alvarez-Puebla, *Angew. Chem. Int. Ed.*, 2012, **51**, 12688–12693.
3 L. Zhang, L. Dai, Y. Rong, Z. Liu, D. Tong, Y. Huang and T. Chen, *Langmuir*, 2015, **31**, 1164–1171.
4 B. Yan, A. Thubagere, W. R. Premasiri, L. D. Ziegler, L. Dal Negro and B. M. Reinhard, *ACS Nano*, 2009, **3**, 1190–1202.
5 F. L. Yap, P. Thoniyot, S. Krishnan and S. Krishnamoorthy, *ACS Nano*, 2012, **6**, 2056–2070.
6 H. I. Park, S. Lee, J. M. Lee, S. A. Nam, T. Jeon, S. W. Han and S. O. Kim, *ACS Nano*, 2014, **8**, 10305–10312.
7 P. N. Njoki, I.-I. S. Lim, D. Mott, H.-Y. Park, B. Khan, S. Mishra, R. Sujakumar, J. Luo and C.-J. Zhong, *J. Phys. Chem. C*, 2007, **111**, 14664–14669.
8 S. Link and M. A. El-Sayed, *J. Phys. Chem. B*, 1999, **103**, 4212–4217.
9 T. Kim, C.-H. Lee, S.-W. Joo and K. Lee, *J. Colloid Interface Sci.*, 2008, **318**, 238–243.
10 R. W. Taylor, R. Esteban, S. Mahajan, R. Coulston, O. A. Scherman, J. Aizpurua and J. J. Baumberg, *J. Phys. Chem. C*, 2012, **116**, 25044–25051.
11 N. G. Khlebtsov, L. A. Dykman, Y. M. Krasnov and A. G. Mel'nikov, *Colloid J.*, 2000, **62**, 765–779.
12 B. C. Mei, E. Oh, K. Susumu, D. Farrell, T. J. Mountziaris and H. Mattoussi, *Langmuir*, 2009, **25**, 10604–10611.
13 M. H. Stewart, K. Susumu, B. C. Mei, I. L. Medintz, J. B. Delehanty, J. B. Blanco-Canosa, P. E. Dawson and H. Mattoussi, *J. Am. Chem. Soc.*, 2010, **132**, 9804–9813.
14 K. K. Caswell, J. N. Wilson, U. H. F. Bunz and C. J. Murphy, *J. Am. Chem. Soc.*, 2003, **125**, 13914–13915.
15 J. J. Storhoff, A. A. Lazarides, R. C. Mucic, C. A. Mirkin, R. L. Letsinger and G. C. Schatz, *J. Am. Chem. Soc.*, 2000, **122**, 4640–4650.
16 K. Niikura, N. Iyo, T. Higuchi, T. Nishio, H. Jinnai, N. Fujitani and K. Ijiro, *J. Am. Chem. Soc.*, 2012, **134**, 7632–7635.
17 A. N. Shipway, M. Lahav, R. Gabai and I. Willner, *Langmuir*, 2000, **16**, 8789–8795.
18 K. A. Huynh and K. L. Chen, *Environ. Sci. Technol.*, 2011, **45**, 5564–5571.
19 A. M. El Badawy, K. G. Scheckel, M. Suidan and T. Tolaymat, *Sci. Total Environ.*, 2012, **429**, 325–331.
20 Z. Zhang, S. Maji, A. B. da F. Antunes, R. De Rycke, Q. Zhang, R. Hoogenboom and B. G. De Geest, *Chem. Mater.*, 2013, **25**, 4297–4303.
21 J. Zhou, R. Sedev, D. Beattie and J. Ralston, *Langmuir*, 2008, **24**, 4506–4511.
22 D. Klotsa and R. L. Jack, *Soft Matter*, 2011, **7**, 6294.
23 D. Zámbó, G. Z. Radnóczi and A. Deák, *Langmuir*, 2015, **31**, 2662–2668.
24 B.-K. Pong, J.-Y. Lee and B. L. Trout, *Langmuir*, 2005, **21**, 11599–11603.
25 D. V. Leff, L. Brandt and J. R. Heath, *Langmuir*, 1996, **12**, 4723–4730.
26 A. Kumar, S. Mandal, R. Pasricha, A. B. Mandale and M. Sastry, *Langmuir*, 2003, **19**, 6277–6282.
27 A. H. Pakiari and Z. Jamshidi, *J. Phys. Chem. A*, 2010, **114**, 9212–9221.

28 K. Yoshimoto, M. Nozawa, S. Matsumoto, T. Echigo, S. Nemoto, T. Hatta and Y. Nagasaki, *Langmuir*, 2009, **25**, 12243–12249.
29 J. Turkevich, P. C. Stevenson and J. Hillier, *Discuss. Faraday Soc.*, 1951, **11**, 55.
30 W. Haiss, N. T. K. Thanh, J. Aveyard and D. G. Fernig, *Anal. Chem.*, 2007, **79**, 4215–4221.
31 T. L. Doane, C.-H. Chuang, R. J. Hill and C. Burda, *Acc. Chem. Res.*, 2012, **45**, 317–326.
32 D. Zopes, B. Stein, S. Mathur and C. Graf, *Langmuir*, 2013, **29**, 11217–11226.
33 L. Cheng, J. Song, J. Yin and H. Duan, *J. Phys. Chem. Lett.*, 2011, **2**, 2258–2262.
34 A. Sánchez-Iglesias, M. Grzelczak, T. Altantzis, B. Goris, J. Pérez-Juste, S. Bals, G. Van Tendeloo, S. H. Donaldson, B. F. Chmelka, J. N. Israelachvili and L. M. Liz-Marzán, *ACS Nano*, 2012, **6**, 11059–11065.
35 Y. Xia, T. D. Nguyen, M. Yang, B. Lee, A. Santos, P. Podsiadlo, Z. Tang, S. C. Glotzer and N. A. Kotov, *Nat. Nanotech.*, 2011, **6**, 580–587.

Perturbation induced directed self-assembly of amino PEGylated gold nanoparticles: kinetics of aggregation and cluster structure.